Liquid Crystalline Polymers in Good Nematic Solvents: Free Chains, Mushrooms, and Brushes

D. R. M. Williams*,† and A. Halperin‡

Laboratoire de Physique de la Matière Condensée,§ Collège de France, 75231 Paris Cedex 05, France, and Department of Materials, University of California, Santa Barbara, California 93106

Received February 10, 1993; Revised Manuscript Received May 4, 1993

ABSTRACT: The swelling of main chain liquid crystalline polymers (LCPs) in good nematic solvents is theoretically studied, focusing on brushes of terminally anchored, grafted LCPs. The analysis is concerned with long LCPs, of length L, with $n_0 \gg 1$ hairpin defects. The extension behavior of the major axis, $R_\parallel$, of these ellipsoidal objects gives rise to an Ising elasticity with a free energy penalty of $F_{el}(R_\parallel)/kT \approx n_0 - n_0(1 - R_\parallel^2/L^2)^{1/2}$. The theory of the extension behavior enables the formulation of a Flory type theory of swelling of isolated LCPs yielding $R_\parallel \sim \exp(2U_h/5kT)N^{3/5}$ and $R_\perp \sim \exp(-U_h/10kT)N^{3/5}$, with N the degree of polymerization and U_h the hairpin energy. It also allows the generalization of the Alexander model for polymer brushes to the case of grafted LCPs. The behavior of LCP brushes depends on the alignment imposed by the grafting surface and the liquid crystalline solvent. A tilting phase transition is predicted as the grafting density is increased for a surface imposing homogeneous, parallel anchoring. A related transition is expected upon compression of a brush subject to homeotropic, perpendicular alignment. The effect of magnetic or electric fields on these phase transitions is also studied. The critical magnetic/electric field for the Frederiks transition can be lowered to arbitrarily small values by using surfaces coated by brushes of appropriate density.

I. Introduction

Thermotropic liquid crystalline polymers (LCPs) are often soluble in nematic solvents.[1-3] Main chain LCPs, consisting of mesogenic monomers joined by flexible spacer chains, are typically soluble in the monomeric liquid crystals. While solutions of polymers in isotropic solutions were extensively studied,[4] little is known of the behavior of LCPs dissolved in nematic solvents. This paper is concerned mainly with one aspect of the *interfacial* behavior of these solutions: An Alexander type theory[5] of flat *tethered layers* of terminally grafted LCPs. Two regimes are considered. In the low grafting density, "mushroom", regime the chains do not overlap. In this regime the configurations of the LCPs are essentially indistinguishable from those of free chains. The "brush" regime is characterized by a high grafting density and pronounced interpenetration of the LCPs. In both cases the layers are immersed in a *good nematic* solvent of low molecular weight. The LCPs are assumed to be monodispersed with a polymerization degree, N, which is sufficiently large so that the trajectories of the LCP exhibit *hairpin* defects,[6-18] i.e., abrupt reversals in the direction of the chain (Figure 1a). We aim to understand the swelling equilibrium of the isolated mushrooms and of the brush, that is, the dimensions of the isolated chains and the thickness, H, of the brush. As we shall see the dimensions of both systems exhibit an exponential temperature, T, dependence in addition to the N dependence. The behavior of the brush is also influenced by other factors: the grafting density, the orientation imposed on the nematic liquid at the surface, and the presence of external fields. As we shall discuss, in certain cases the brush is expected to undergo a tilting phase transition.

The distinctive features of these systems are due to the coupling between the nematic order and the configurations of the LCPs. Roughly speaking the trajectories of the chains follow the nematic field and vice versa. This has two consequences: (i) The configurations of the LCPs are *anisotropic*. In a coarse grained fashion the LCPs may be viewed as prolate ellipsoids. As we shall see the elastic behavior of the LCP is also anisotropic. (ii) The major axis of the ellipsoid is aligned with the nematic field. Consequently, it is possible to impart an absolute spatial *orientation* to the LCP by orienting the surrounding solvent. This may be done by applying a magnetic or an electric field. Alternatively, it is possible to utilize "anchoring", i.e., alignment of the liquid crystal by surfaces which imposes a specific orientation at the interface.

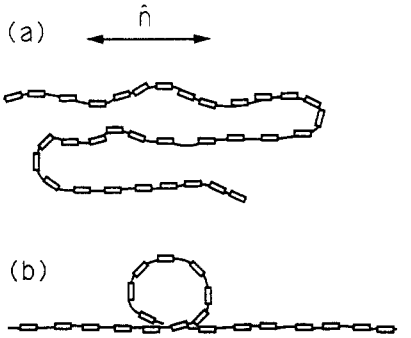

Figure 1. Two types of defects which can occur in oriented polymers. (a) A two-hairpin configuration in a nematic chain. Here the chain is assumed to consist of nematic mesogens separated by flexible spacers. The nematic director is specified by $\hat{\mathbf{n}}$. (b) A roller, which can occur either in a dipolar chain in an electric field or in a strongly stretched nematic chain.

In certain respects the swelling behavior of free LCP is rather familiar. Both major and minor axes of the LCP, $R_\parallel$ and $R_\perp$, exhibit a Flory scaling behavior $R_\parallel \sim R_\perp \sim N^{3/5}$.[4,19,20] The anisotropy of the chains is due to prefactors which result in exponential temperature dependence. However, the temperature dependence of the two dimensions is different. $R_\parallel$ shrinks with increasing T while $R_\perp$ grows. The two dimensions are observable in samples of free chains aligned by an external field.[21-23] Similar measurements are possible for tethered LCPs in the mushroom regime when the chains are grafted to a surface

† Collège de France.
‡ University of California.
§ Unité Associée no. 792 du CNRS.

0024-9297/93/2226-4208$04.00/0

imposing an appropriate anchoring condition. The thickness of the tethered LCP brush, H, retains the Alexander scaling behavior with respect to N and the area per chain, Σ, $H \sim N\sigma^{-1/3}$.[5] As in the mushroom regime, H exhibits an exponential T dependence typical of LCPs with hairpins. Again, H is strongly influenced by the anchoring conditions. When the alignment of the nematic solvent is parallel to the surface, H is much smaller. Furthermore, in this case the brush is expected to undergo a *tilting phase transition* as Σ is decreased:[24] The interpenetration of the chains is enhanced when Σ shrinks. This effect is much stronger when the major axis of the LCP is parallel to the surface. Tilting the major axis with respect to the surface is thus beneficial as a way of weakening the overlap between the chains and thus lowering the interaction free energy. At the same time tilt is penalized by the distortion free energy of the nematic medium. The interplay of these two factors results, within our picture, in a second-order phase transition. The onset of this transition is controlled by Σ as well as by confinement and the application of external fields. A related tilting transition is expected in compressed brushes when the surface imposes a perpendicular orientation of the nematic medium. The resulting transition is reminiscent of the familiar Frederiks transition.[25-27] In this transition a field is applied which is antagonistic to the anchoring conditions. Below the critical field strength there is no nematic distortion. Above this threshold some of the molecules align with the field, and a distortion of the director takes place. A similiar tilting transition is also expected in solutions of free LCPs when confined between two surfaces imposing homeotropic anchoring.[28,29] In this case as well the driving force is due to the deformation penalty of the LCPs rather than to the action of an external field.

The behavior of tethered LCPs is of interest from a number of view points. Tethered LCPs may be used to control the anchoring behavior of surfaces. Furthermore, as we shall see, under proper conditions LCP brushes can modify the response of nematic liquid crystals to external fields. This last feature opens a new avenue for improving the performance of nematic working fluids in display devices.[30] The tilting transition in free brushes is of interest in its own right as a form of *anchoring transition*[31] since transitions of this type are not well understood microscopically. The confinement induced tilting is of interest because of its similarity to the Frederiks transition. From the polymer science perspective, tethered LCPs exhibit novel features.[32,33] The two most noteworthy features are the role of tilt and the occurrence of tilting phase transitions. These are but a few examples of the rich behavior expected from LCPs in nematic solvents.

The paper is organized as follows, section II is a reminder of the main properties of monomeric and polymeric liquid crystals. In section III we describe the theory for stretching of nematic chains along the nematic director. This is compared with the stretching energy of ordinary isotropic chains. We then present a Flory type theory for the swelling of a main chain LCP in a good nematic solvent. The presentation follows, with certain elaboration, the discussion of ref 34. The case of a brush grafted to a surface imposing homeotropic, perpendicular anchoring is discussed in section IV. The discussion includes a comparison to the isotropic case for weak and strong stretching, where finite extensibility becomes important. Also studied is the case of chains tethered to surface characterized by homogeneous, parallel, anchoring. A tilting phase transition is predicted for large enough grafting densities.[24] Section V is devoted to the analysis of the effect of compression on this tilting transition. Section VI decribes, in detail, the effect of grafted brushes on the Frederiks transition. In particular, we show that a grafted brush can reduce the field threshold for nematic distortion to an arbitrarily small value.

II. Background: Nematic Solvents and Liquid Crystalline Polymers

The solvents considered in this paper are thermotropic, uniaxial, nematic liquid crystals.[25-27] These are typically formed by cylindrical molecules comprising of an aromatic core decorated by hydrocarbon tails. At high temperatures these materials form a liquid phase with no long range order. As the temperature is lowered the system undergoes a phase transition to a nematic state characterized by long range orientational order: The axes of the nematogenic molecules tend to align while their centers of gravity do not show long range order. The parameters specifying the state of the nematic phase are averages taken over small volume elements which are nevertheless large on molecular scale. The two parameters are (i) a unit "headless" vector, $\mathbf{n}$, the director, specifying the single preferred direction of molecular orientation (Only the orientation is of significance. States with $\mathbf{n}$ and $-\mathbf{n}$ are indistinguishable.[35]) and (ii) the order parameter $S = \langle(3\cos^2\theta - 1)\rangle/2$, where θ is the angle between the molecular axes and $\mathbf{n}$, which measures the strength of the alignment. Our interest is confined to strongly oriented nematics, $S \approx 1$, well below the clearing temperature. The macroscopic state of the system is specified by S and by the director field $\mathbf{n}(\mathbf{r})$. The "ground state" of the sample is a perfectly aligned "single crystal". Distortions of $\mathbf{n}(\mathbf{r})$ give rise to an excess free energy density, f_{dis}. The excess distortion free energy density, as obtained from the phenomenological continuum theory, is[25-27]

$$f_{dis} = \frac{1}{2}K_1(\text{div } \mathbf{n})^2 + \frac{1}{2}K_2(\mathbf{n}\cdot\text{curl } \mathbf{n})^2 + \frac{1}{2}K_3(\mathbf{n} \times \text{curl } \mathbf{n})^2 \quad (1)$$

where K_1, K_2, and K_3 are the elastic constants, of order 1×10^{-6} dyn, associated respectively, with the splay, twist, and bend distortions. In our subsequent discussion we resort to the one constant approximation: $K_1 = K_2 = K_3 = K$. Distortions occur when dissimilar orientations are imposed on different regions of the sample. By using eq 1, it is possible to solve for the $\mathbf{n}(\mathbf{r})$ which minimizes the total excess distortion free energy, $F_{dis} = \int f_{dis}\, dV$, while obeying the constraints. It is possible to orient the nematic medium by applying an electric or magnetic field. This effect utilizes the anisotropy of the magnetic susceptibility and the dielectric constant. A nematic can also be oriented by "anchoring", that is, utilizing a surface imposing certain boundary conditions. The two situations considered in the following involve homeotropic and homogeneous anchoring where $\mathbf{n}$ at the interface is respectively perpendicular and parallel to the surface.

The orientational order of the nematic has a 3-fold effect on the LCP solutes: First, the mixing energy of the monomers is modified.[36] Second, the coupling of the LCP trajectory and the nematic field give rise to anisotropic configurations. Finally, the spatial orientation of the LCP can be controlled by aligning the nematic solvent. In turn, the nematic solvent is distorted when the LCP is forced to deviate from the imposed orientation. The first two points, and especially the second, were studied extensively.[6-18] The rest of this section is devoted to a brief summary of the results. Less attention was given to the third point. Some of its ramifications are considered in the following sections.

The effect on the mixing energy may be described phenomenologically. Following Brochard[36] the Flory χ parameter is written as

$$\chi_n = \chi_0 + \chi_1 S^2 \quad (2)$$

χ_0 describes the interactions in the isotropic phase while the second term allows for the effect of the nematic order.[37] For ordinary polymers, which are almost insoluble in nematic solvents, $\chi_1 \approx 1$, while for soluble LCP $\chi_1 \ll 1$. The second virial coefficient is accordingly given by $\upsilon_n = a^3(1-2\chi_n)$. The θ condition within this scheme is specified by $\chi_0 + \chi_1 S^2 = 1/2$: A nematic Θ solvent is obtained from a marginal isotropic solvent.

We will now discuss the configurations of LCP in nematic media.[6] In this section we focus on LCP in a melt of identical chains or in a Θ solvent. The configurations in good solvents will be discussed in the next section. Semiflexible LPCs are pictured as persistent chains of constant length which are flexible enough to be capable of bending. The angular correlations between tangents to the chain decay as $\langle \cos \theta(\delta) \rangle \approx \exp(-\delta/\zeta)$, where $\theta(\delta)$ is the angle between two tangents separated by a distance δ along the contour of the chain. ζ, the persistence length, is related to the chain rigidity, $\epsilon = kT\zeta$. The elastic free energy per unit length of the chain is $(\epsilon/2)(d\theta/ds)^2$, where s is the arc length position along the chain. In an isotropic medium, a LCP of length $L \gg \zeta$ behaves as a random walk of L/ζ steps of length ζ. Accordingly $R_\perp{}^2 = R_\parallel{}^2 = R^2$ and[38,29]

$$R^2 \approx L\zeta \quad (3)$$

In a nematic medium, the LCP experiences an anisotropic molecular field due to a combination of van der Waals attraction and steric repulsive interactions. The Maier–Saupe potential[25-27] provides a phenomenological description of this field. A unit length of the chain experience a field $V(\theta) = a_n S P_2(\cos\theta)$ where a_n is a coupling constant with units of energy/length, $P_2(\cos\theta)$ is a Legendre polynomial of the second order and θ is the angle between the tangent to the chain and **n**. It is important to note the molecular field acts on *both* the nematogenic monomers and the flexible spacer chains. On short length scales, $\delta \ll \zeta$, the LCP behaves as a persistent chain in an isotropic medium. The angular correlations on such scales obey

$$\langle \theta^2 \rangle \approx \delta/\zeta \quad (4)$$

On long length scales, $\Delta \geq \zeta$, the effect of the nematic field is dominant. The probability density of an orientation with a certain θ is

$$P(\theta) \sim \exp(-a_n \Delta S \theta^2/kT) \quad (5)$$

and thus

$$\langle \theta^2 \rangle \approx kT/a_n \Delta S \quad (6)$$

The cross over between the two regimes defines a new length scale, the deflection length[39,40]

$$\lambda \approx (\epsilon/a_n S)^{1/2} \quad (7)$$

and the shorter λ replaces ζ as the angular correlation length. Thus, the nematic field accelerates the decay of the angular correlations while imposing strong alignment with **n**. This is because the chain is, in effect, confined to a conical capillary with deflecting walls. This picture, of an undulating line within a virtual capillary, yields a satisfactory description of the lateral dimensions of the chain, $R_\perp$. Equation 6 reveals that each ζ segment is confined to a conical capillary with a basal radius of λ. The lateral dimensions of the LCP are thus due to a two-dimensional random walk of L/ζ steps of length λ: The change in the step length, from ζ to λ, is a consequence of the bias introduced by the nematic field. Altogether the lateral dimensions of the chain are given by $R_\perp{}^2 \approx (L/\zeta)\lambda^2$. This defines a new length scale

$$l \approx \lambda^2/\zeta \approx kT/a_n S \quad (8)$$

l may be interpreted as the elementary step length of a two-dimensional random walk perpendicular to **n** so that $R_\perp{}^2$ is given by

$$R_\perp{}^2 \approx (L/l)l^2 = Ll \quad (9)$$

The uncertainty in the spatial position of a monomer along the **n** direction is also specified by l. While the "chemical", arc length distance from the chain end is constant, the distance in real space is affected by the thermal undulations of the trajectory. The angle θ between a chain segment of length $\Delta > \lambda$ and **n** fluctuates between 0 and $\langle \theta^2 \rangle^{1/2} \approx (kT/a_n S\Delta)^{1/2}$. Accordingly, the projection on **n** fluctuates between Δ and $\Delta \cos\theta$ and the uncertainty is $\langle \Delta - \Delta \cos\theta \rangle \approx \Delta\langle\theta^2\rangle \approx l$.

The characteristic dimension discussed above may be obtained from energy considerations. Three energies are involved: elastic, nematic, and thermal. The elastic energy ϵ/Δ is of order kT for chain segments of length $\Delta \approx \zeta \approx \epsilon/kT$. The nematic energy, $\Delta a_n S$, is comparable to the elastic energy ϵ/Δ for $\Delta \approx \lambda \approx (\epsilon/a_n S)^{1/2}$. Finally, the nematic energy, $\Delta a_n S$, is of order kT for $\Delta \approx l \approx kT/a_n S$. This last point rationalizes (9) by defining a subdivision of the LCP into segments of length l, comparable to their lateral projection, such that the associated nematic penalty per segment is of order kT. Chain segments of length l play thus the role of blobs defined by a nematic energy rather than by interaction energy.

This picture suggests that the chain is strongly stretched in the direction of **n** so that $R_\parallel \approx L$. This conclusion is valid for relatively short chains. For longer chains one must allow for the contribution thermal excitations known as hairpin defects[6-18] (Figure 1). These are abrupt reversals in the direction of the chain. The dimensions of the bent region, a few λ, are set by the balance of two terms: The elastic penalty, which favors gradual bend, and the nematic contribution which promotes an abrupt change of direction so as to minimize the deviation from the alignment with **n**. Each hairpin is endowed with an energy, U_h, of order ϵ/λ

$$U_h \approx (a_n S \epsilon)^{1/2} \quad (10)$$

Because hairpins are marginally stable entities, their lifetime is expected to be long. It is thus possible to treat them as quasiparticles. When the concentration of the hairpins is low, a chain populated by n hairpins may be viewed as a one-dimensional regular solution. The system is inscribed on a lattice with a unit cell l set by the uncertainty in the spatial position of the hairpins. The free energy of a chain is thus

$$F = nU_h + nkT \ln(nl/L) \quad (11)$$

where nl/L is the length fraction of the hairpin solutes. The average number of hairpins in equilibrium, n_0, is found by minimizing F with respect to n

$$n_0 = (L/l)\exp(-U_h/kT) \quad (12)$$

When $n_0 \gg 1$ the chain performs a one-dimensional random walk of n_0 steps of average length L/n_0 in the direction of

n. The average dimension of the chain along the **n** direction, $R_{\|0}$, is thus

$$R_{\|0}^2 \approx L^2/n_0 = Ll \exp(U_h/kT) \quad (13)$$

and the anisotropy of the chain is characterized by $R_{\|0}^2/R_{\perp 0}^2 \approx \exp(U_h/kT)$. Altogether we may distinguish two limits. For $L < l\exp(U_h/kT)$, when the hairpin population is essentially zero, the chain dimensions are $R_\| \approx L$ and $R_\perp^2 \approx Ll$. In the opposite limit, $L \gg l\exp(U_h/kT)$, $n_0 \gg 1$ so that $R_\|^2 \approx L^2/n_0$ and $R_\perp^2 \approx Ll$. In this case the lateral dimensions of the chains are determined by the undulations of their trajectories while $R_\|$ is set by the hairpins. The superposition of these two contributions gives rise to the roughly ellipsoidal objects discussed in the introduction. Our following discussion is limited to the second regime.

The theoretical picture summarized above dates from the seminal paper of de Gennes.[39,41] Experimental verification was slow to materialize. The most detailed probe of macromolecular configurations, small angle neutron scattering (SANS), is difficult to implement in this case:[22,23,42] Since main chain LCPs are synthesized by condensation polymerization, it is difficult to obtain samples with high polymerization degrees and low polydispersity. This difficulty is compounded by the necessity to deutrate the polymers and to obtain uniform mixture of the deutrated and hydrogenated chains. Finally, many of the main chain LCPs are aromatic polyesters. These are subject to transesterification reactions involving chains scission followed by recombination of the chain fragments. This leads to interchange of chain segments between different LCPs. In turn, this causes redistribution of deutrated monomers among the chains as well as widening of the molecular weight distribution. Both effects make for difficulties in interpretation of the SANS data. Nevertheless, qualitative agreement with theory was reported by D'Allest et al.[21] and in a later work by Arrighi et al.[22] Recent SANS experiment by Li et al.[23] probed melts of main chain LCPs under conditions ensuring negligible transesterification effects. This study demonstrate the existence of hairpins in long LCPs and the expected trend in the temperature dependence of n_0.

One should also note that "hairpins" stabilized by chemical interactions are commonly identified in the configurations of proteins.[43] These structures are stabilized energetically rather than entropically as in our case. Also, protein hairpins are permanent features, not excitations.

III. Stretching and Swelling

As we have seen, the configurations of long LCPs result from the superposition of two random walk components. $R_{\perp 0}$ is determined by a two-dimensional random walk with a constant step l, traceable to the undulations of the chain trajectory. On the other hand, $R_{\|0}$ is determined by a one-dimensional random walk of n_0 steps of length L/n_0, which is due to the presence of hairpins. The involvement of random walk components suggests a Gaussian stretching behavior for both $R_\perp$ and $R_\|$. Indeed, for the lateral component, $R_\perp$, the stretching free energy is expected to follow the familiar Gaussian form

$$F_{el}(R_\perp)/kT \approx R_\perp^2/R_{\perp 0}^2 \quad (14)$$

The extension behavior of $R_\|$ is more complex.[7,18,24] While weak extension may result only in spatial rearrangement of the hairpins, strongly stretched chains are expected to shed hairpins. Stretching $R_\|$ can thus lower the number of steps, n, and increase their average length, L/n. This situation is outside the framework of the traditional theory of chain elasticity. An alternative approach is suggested by the effect of tension on a chain with hairpins. The hairpins divide the chain into two types of segments: + segments, which are favored by the tension, and − segments which are penalized by it. If we imagine moving from the origin of the chain toward its end, the motion in the + segments is forward directed in space while the motion in the − segments is directed backward. The external energy due to the tension **f** is

$$-\mathbf{f}\cdot\mathbf{R}_\| = -f(s_1 - s_2 + s_3 - \ldots + s_n) \quad (15)$$

where s_i is the length of the ith segment. The application of tension results in shrinking of the − segments and in growth of the + segments. This picture suggests an analogy between the stretching behavior of LCP with hairpins and the magnetization of a one-dimensional Ising model.[44,45] In particular, the + and − segments correspond respectively to domains of up and down spins. The hairpins are analogous to domain boundaries with a boundary energy U_h. A hairpin is situated at the bond, of length l between two adjacent lattice sites. Since a bond can support at most a single hairpin, the maximum occupancy of the chain is $N-1$, where $N = L/l$. Hairpins behave thus as fermions.[46] The tension, f, is analogous to the magnetic field while the magnetization corresponds to the end to end distance, $R_\|$. This mapping is especially transparent when the one-dimensional Ising chain is described in terms of the domain boundaries.[44] However, typically one obtains the free energy and magnetization for a given field or, in our case, F and $R_\|$ for a given f. Since our ultimate aim is the construction of a Flory type theory of swelling, we need $F_{el}(R_\|)$ rather than $F_{el}(f)$. It is instructive to derive $F_{el}(R_\|)$ from a different point of view. The partition function of LCP chain with n hairpins and a given $R_\|$ is

$$Z = \exp(-nU_h/kT)W_+W_- \quad (16)$$

where $W_+(W_-)$ is the statistical weight of the +(−) segments. W_+ and W_- count the configurations yielding + (−) domains of total length $L_\pm = N_\pm l$ such that $L_+ - L_- = R_\|$ and $L_+ + L_- = L$. These configurations are obtained by different arrangements of N l bonds and n hairpins. For $n \gg 1$ we have, approximately, $n/2$ − segments and $n/2$ + segments. The combinatorial problem involved concerns the number of ways in which $N_\pm$ indistinguishable objects can be placed into $n/2$ boxes. Accordingly[47]

$$W_\pm = \left(N_\pm + \frac{n}{2}\right)!/N_\pm!\frac{n}{2}! \quad (17)$$

The corresponding free energy, $F = -kT \ln Z$, is thus

$$F(R_\|)/kT = nU_h + n\ln\frac{n}{2} - \sum_{i=+-}\left[\left(N_i + \frac{n}{2}\right)\ln\left(N_i + \frac{n}{2}\right) - N_i \ln N_i\right] \quad (18)$$

where $N_\pm = (L \pm R_\|)/2l$. The equilibrium n for a given $R_\|$ is obtained by minimizing $F(R_\|)$ with respect to n. Outside the strong stretching regime, when both n and N_- are small, we may assume $n \ll N_\pm$. This yields

$$n = \left(\frac{L^2 - R_\|^2}{l^2}\right)^{1/2}\exp(-U_h/kT) = n_0\left(1 - \frac{R_\|^2}{L^2}\right)^{1/2} \quad (19)$$

The middle expression differs from n_0 in that the geometric mean $(L_+L_-)^{1/2}$ replaces L. The combination of (18) and

$\partial F/\partial n = 0$ yields $F(R_\parallel)$ for the annealed chain, i.e., for an equilibrated hairpin population

$$F(R_\parallel)/kT = -\sum_{i=+-} N_i \ln (1 - n/2N_i) \tag{20}$$

When $n \ll N_\pm$ and the undistorted chain serves as a reference state, this leads to

$$F(R_\parallel)/kT = n_0 - n \tag{21}$$

and the restoring force is accordingly

$$f/kT = (R_\parallel/l)(L^2 - R_\parallel^2)^{-1/2} \exp(-U_h/kT) = (R_\parallel/R_{\parallel 0}^2)(1 - R_\parallel^2/L^2)^{-1/2} \tag{22}$$

For weak extensions, when $(1 - R_\parallel^2/L^2)^{1/2} \approx 1$, the chain exhibits Gaussian behavior, $F_{el}(R_\parallel)/kT \approx R_\parallel^2/R_{\parallel 0}^2$ and $n \approx n_0$. The $(1 - R_\parallel^2/L^2)^{1/2}$ "saturation" factor becomes important for strong stretching, when $n \ll n_0$ and the finite extensibility of the chain must be taken into account. In this regime the saturation factor gives rise to a divergence in f. For flexible chains, this regime is often described by the "inverse Langevin" expression[19,20]

$$F_{el}/kT = \int_0^R \mathcal{L}^*(x/Na)\, dx \tag{23}$$

and

$$fa/kT = \mathcal{L}^*(R/Na) \tag{24}$$

where a is the monomer size and $\mathcal{L}^*$ is the inverse of the Langevin function $\mathcal{L}(x) = \coth x - 1/x$. The two force laws differ in their precise form for intermediate extensions and in their divergence behavior. At small extensions both force laws give a linear "Gaussian" behavior, $f/kT \sim R_\parallel/R_{\parallel 0}^2$. However, for a given extension and degree of polymerization the restoring force associated with Ising elasticity is much weaker. This is because PLCs in nematic medium have a much larger unperturbed parallel radius of gyration, the ratio being $R_{\parallel 0}^2(\text{Nem})/R_{\parallel 0}^2(\text{Iso}) \sim (l/a)\exp(U_h/kT) \gg 1$. At large extensions both force laws diverge, but in the isotropic case the force diverges as $\propto \delta^{-1}$ whereas in the nematic case it diverges as $\delta^{-1/2}$, where $\delta \equiv 1 - R_\parallel/L$. The differences between the isotropic and nematic cases are not unexpected. Equation 23 corresponds to the alignment of a constant number of noninteracting dipoles by an electric field. Each dipole is analogous to a Kuhn segment and the field plays the role of tension. This situation is clearly different from the magnetization of an Ising chain of interacting spins or the stretching of a chain with a variable number of Kuhn segments. There is one other major difference between the Ising and the inverse Langevin elasticities. To fully stretch an Ising chain takes a finite amount of energy, $n_0 kT$, whereas an infinite amount of energy is required to stretch an "inverse Langevin" chain. This difference arises because the Ising elasticity accounts for the effect of the hairpins but does not allow for the contribution of chain undulations. Removing the hairpins does not eliminate the undulations, and removal of the chain undulations would, indeed, require an infinite stretching energy.

We have argued that the Ising stretching energy for a given extension is much smaller than that for an isotropic chain. Furthermore, the crossover between weak and strong stretching occurs at a much lower energy threshold for the Ising chain. In both cases this threshold occurs at $R_\parallel \sim L$ and the energy required to reach this threshold is $\sim kTL^2/R_\parallel^2$. However, since $R_{\parallel 0}^2(\text{Nem})/R_{\parallel 0}^2(\text{Iso}) \gg 1$, we expect non-Gaussian effects to be reached much faster and be much more important in the case of LCP in nematic media.

Our above presentation of the Ising elasticity follows the discussion of ref 34. The essential features were noted earlier by Kamien *et al.*[18] in the context of a field theoretical description of directed polymers. The concept is also implicit in the work of Gunn and Warner.[7] However, the general idea of the Ising elasticity is actually much older. The stretching elasticity of biopolymers was already discussed in these terms by Hill in 1960.[48]

Our discussion of the deformation behavior of LCPs in nematic media is applicable while l and λ are determined by the nematic field. This regime survives while the strain energy is a small perturbation, that is, $fl \ll kT$. When f is larger or comparable to kT/l, a new regime emerges. In this regime the tension replaces the nematic field in determining the chain structure. In particular, the deflection length in the strong extension regime is $\lambda_f \approx (\epsilon/f)^{1/2}$ as specified by the balance $\epsilon/\lambda_f \approx \lambda_f f$. Similarly, l is replaced by $l_f \approx kT/f$ as defined by $fl_f \approx kT$. Accordingly, the strongly stretched LCP is expected to have $R_\parallel \approx L$, $R_\perp^2 \approx (L/l_f)^2 l_f \approx fL^2/kT$ and its hairpin population is, essentially, zero. This regime is analogous to the Pincus regime in strongly stretched isotropic chains.[4] Also, at such strong stretching the extensional field controls the allowed defects. Accordingly, the hairpins are no longer the important excitation, and a new defect, the "roller" [49] (Figure 1b), becomes important. In the vicinity of this regime there is a whole menagerie of defects intermediate between hairpins and rollers,[49] and a complete discussion of the extensional behavior is complicated.

Monomer–monomer interactions are strongly repressed in short, $L < l \exp(U_h/kT)$, hairpin-free LCPs. In the opposite limit, $n_0 \gg 1$, the hairpins promote such interactions and, as a result, swelling. A modified Flory theory provides a simple description of the swelling behavior.[34] As in the case of flexible chains in isotropic solvents, the swelling reflects an interplay of the interaction free energy, F_{int}, and the elastic free energy F_{el}. Two modifications are necessary: In the standard theory $F_{int}/kT \approx v_0 N^2/R^3$ where, in our notation, $v_0 = a^3(1 - 2\chi_0)$. To allow for the effect of the nematic order, v_0 is replaced by v_n. Furthermore, the volume of the coil, R^3, is now given by $R_\perp R_\parallel^2$ to account for the anisotropicity of the LCP. Finally, the single elastic term in the standard theory, $F_{el}/kT \approx R^2/R_0^2$ is replaced by two terms, $F_{el}(R_\parallel)$ and $F_{el}(R_\perp)$. In principle $F_{el}(R_\parallel)$ has the Ising form. However, as shown below, for isolated chains the stretching is not very strong, $R_\parallel \ll L$, and the Ising form reduces to a Gaussian one. Yet, as noted previously, the two terms are different. $F_{el}(R_\parallel)/kT \approx R_\parallel^2/R_{\parallel 0}^2$ is much weaker than $F_{el}(R_\perp)/kT \approx R_\perp^2/R_{\perp 0}^2$ because $R_{\parallel 0} \gg R_{\perp 0}$. Altogether, the free energy of a single LCP is

$$F_{chain}/kT = v_n \frac{N^2}{R_\perp^2 R_\parallel} + \frac{R_\perp^2}{Ll} - n_0\left(1 - \frac{R_\parallel^2}{L^2}\right)^{1/2} \tag{25}$$

and the equilibrium condition, $\partial F/\partial R_\parallel = \partial F/\partial R_\perp = 0$, yields

$$R_\parallel = (l/a)^{4/5} \exp(2U_h/5kT) R_F \tag{26}$$

$$R_\perp = (l/a)^{7/10} \exp(-U_h/10kT) R_F$$

where $R_F = v_n^{1/5} N^{3/5} a^{2/5}$ is the Flory radius of a flexible chain. A prerequisite for the assumed Gaussian elasticity is that $R_\parallel \ll L$. Since $R_\parallel \approx n_0^{-2/5} v_n^{1/5} N l^{2/5}$ implies $v^{1/2} l a^{-5/2} \ll n_0$, the left-hand side of this inequality is somewhat larger than unity. Accordingly, our theory is applicable when many hairpins are present; i.e., $n_0 \gg 1$, the chain supports many hairpins in a θ solvent. We note that both

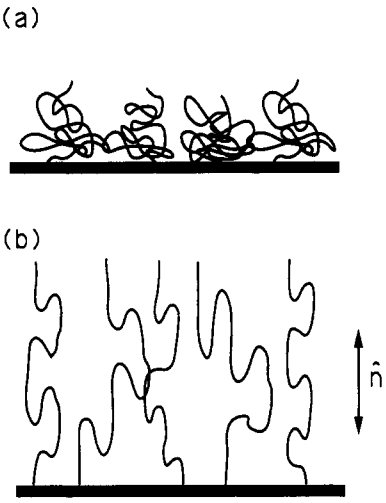

Figure 2. (a) An isotropic polymer brush in an isotropic solvent. (b) A homeotropically anchored nematic brush in a nematic solvent. By lowering the temperature through the isotropic to nematic regime, we can go from (a) to (b). There will then be a large increase in the brush thickness. In both cases the Alexander model is depicted; i.e. all the ends are located at the brush surface.

$R_\parallel$ and $R_\perp$ exhibit the familiar $N^{3/5}$ scaling behavior. The anisotropy of the chain is due to the different exponential weighting factors. These also give rise to a distinctive temperature dependence: Both $R_\parallel$ and $R_\perp$ depend exponentially on T. Furthermore, $R_\parallel$ *shrinks* with increasing T while $R_\perp$ *grows*. For LCPs in the melt state $R_{\parallel 0}$ and $R_{\parallel 0}$ scale as $N^{1/2}$ and only $R_\parallel$ exhibits such exponential T dependence. In marked distinction, the temperature dependence of the dimensions of flexible chains in isotropic media is nonexponential and isotropic.[4] Within this Flory type approach, free chains and sparsely grafted mushrooms are indistinguishable. However, in the mushroom case it is necessary to allow for the effect of anchoring conditions. $R_\parallel$ is perpendicular to the surface for homeotropic anchoring and parallel for the homogeneous case.

IV. Grafted LCP: Free Brushes

The crossover between the mushroom and the brush regimes is straightforward to analyze in the case of homeotropic anchoring (Figure 2). When Σ is lowered past the overlap theshold, $\Sigma^* \approx R_{\perp 0}^2$, the chains begin to stretch outward. This lowers their interaction free energy at the price of an elastic penalty. The analysis of the case of homogeneous anchoring is more complex because of the role of chain tilt and is discussed later in this section. We begin with a discussion of the simpler, homeotropic case within the framework of the Alexander model.[5,32,33] It is based on two assumptions: (i) The chains are uniformly stretched, with their free ends straddling the outer edge of the brush at height H. (ii) The monomer concentration profile is steplike; i.e., the monomer volume fraction within the layer is $\phi = Na^3/\Sigma H$. The free energy per chain consists, again, of two terms. An interaction free energy, F_{int}, and an elastic penalty term, F_{el}. The interaction term is similar to the one used in (25) with the caveat that the volume per coil is now ΣH so that $F_{int}/kT \approx v_n N^2/\Sigma H$. Only the "Ising" elastic term is involved in the case of homeotropic anchoring, when $\mathbf{n}$ and $R_\parallel$ are perpendicular to the surface. Altogether, the free energy per chain, F_{chain}, is

$$F_{chain}/kT = v_n N^2/\Sigma H - n_0(1 - H^2/L^2)^{1/2} \quad (27)$$

For $\Sigma^* > \Sigma \gg a^2$ when $H \ll L$ and $F_{el}/kT \approx H^2/R_{\parallel 0}^2$ the equilibrium condition, $\partial F/\partial H = 0$, yields

$$H_{\perp 0} \approx v_n^{1/3} N(al/\Sigma)^{1/3} \exp(U_h/3kT) \quad (28)$$

For higher coverages it is necessary to allow for the finite extensibility of the LCP and the full expression for the Ising elasticity must be used. Furthermore, in this regime the monomer volume fraction is higher, and the approximation of the interaction free energy by the binary term is insufficient. A better approximation for F_{int} is provided by the Flory mixing free energy

$$F_{int}/KT = \Sigma H a^{-3}[(1 - \phi)\ln(1 - \phi) + \chi_n \phi(1 - \phi)] \quad (29)$$

where the Brochard χ_n replaces the standard Flory χ parameter. The combination of these two terms yields the following free energy per chain

$$F_{chain}/NkT = -\omega(1 - t^2)^{1/2} + (\rho t)^{-1}(t - \rho)[\chi_n \rho + t \log(1 - \rho/t)] \quad (30)$$

where $t \equiv H/L \leq 1$ is a dimensionless brush height and $\rho \equiv a^2/\Sigma \leq 1$ is a dimensionless coverage or area fraction of grafting sites. $\omega \propto (a/l)\exp(-U_h/kT) \ll 1$ compares the parallel extent of the chain in the isotropic and nematic cases, i.e., $\omega \sim R_{\parallel 0}^2(\text{Iso})/R_{\parallel 0}^2(\text{Nem})$. Upon minimizing with respect to t, we obtain the equilibrium condition

$$\omega \rho t^3 + (1 - t^2)^{1/2}[\rho t + t^2 \ln(1 - \rho/t) + \chi_n \rho^2] = 0 \quad (31)$$

It is interesting to compare this with the case of an isotropic brush.[50] There, the equation for the height of a brush immersed in an athermal solvent, $\chi = 0$, is

$$t + \mathcal{L}(t^{-1} + \rho^{-1} \ln(1 - \rho t^{-1})) = 0 \quad (32)$$

In the close packing limit, $\rho = 1$, the chains are fully extended and $t = 1$ for both the isotropic and LCP brushes. However the LCP brush approaches full stretching much more rapidly than an isotropic brush (Figure 3). This is a consequence of the weaker force law for parallel stretching.

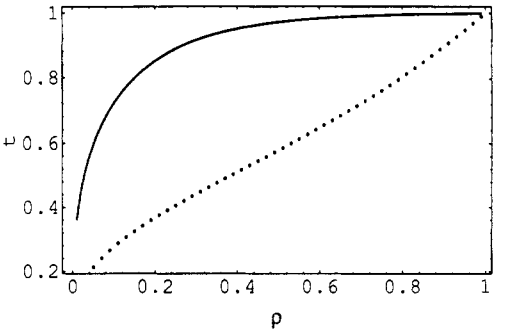

Figure 3. Dimensionless brush height t versus coverage for a brush of ordinary isotropic polymers (dotted line) and a homoetropically anchored LCP brush (full line) with $\omega = 0.1$. In both cases $\chi = 0$. Because the restoring force for the LCP is much weaker, it gains 80% of its full extension when the coverage is only 20%. A similar extension for an isotropic brush occurs only for very high coverages.

The theoretical analysis of a brush grafted onto a surface imposing homogeneous anchoring is more complicated. We first need to make some remarks on the grafting of the polymers to the surface. If the grafting takes place in an isotropic medium, then the distance between grafting sites is independent of in-plane direction. If however, the grafting is carried out in a nematic medium, then two different site-to-site distances, $x_\parallel$ and $x_\perp$, are expected (Figure 4a) with $x_\parallel > x_\perp$. For simplicity we assume here grafting in an isotropic medium so that $x_\perp = x_\parallel = \Sigma^{1/2}$. We also require an alignment of the homogeneous anchoring

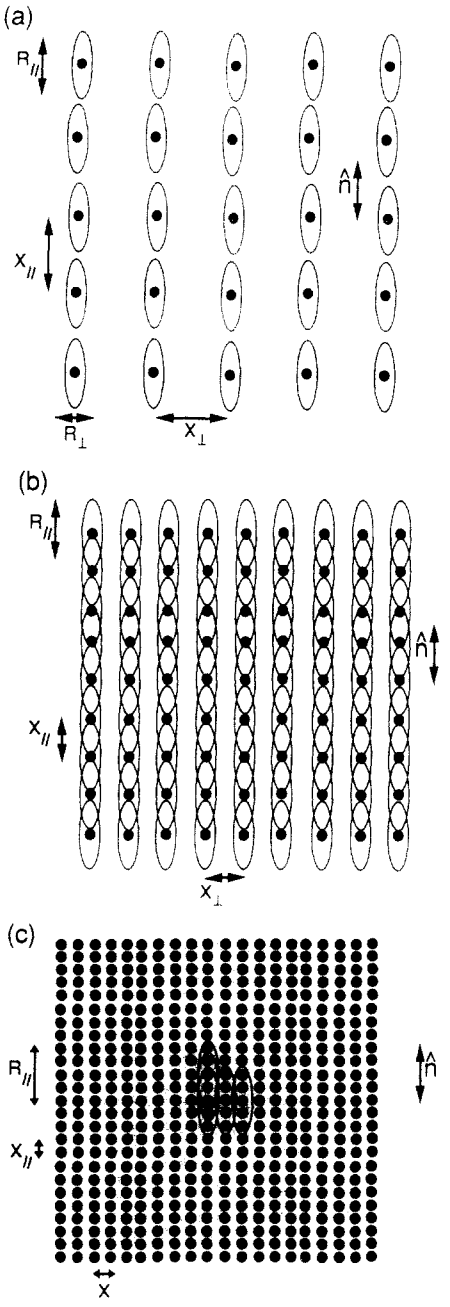

Figure 4. Three regimes distinguished in an untilted, homogeneously anchored brush as seen from above. In the general case the grafting distances $x_\perp$ and $x_\parallel$ may be different, but here they are depicted as being identical. Each chain is represented as an ellipse with its long axis along the nematic director. For clarity only a few chains are shown. The grafting sites are shown as solid circles. (a) The mushroom, low coverage regime. In this regime none of the chains overlap. (b) A brush with area per headgroup $\Sigma < R_\parallel^2$, where the chains overlap in the parallel direction giving rise to a series of parallel semicylindrical brushes. (c) A brush at larger grafting density, so that $\Sigma < \Sigma^*$. In this case the chains overlap in both the parallel and perpendicular directions. As a result only perpendicular swelling is beneficial.

so that **n** is not only parallel to the surface but also oriented in a particular direction along the surface. For simplicity we place the grafting sites on a square lattice with a lattice constant of $\Sigma^{1/2}$. This last assumption should not affect the discussion of low and high grafting densities. However, it should be scrutinized with care for intermediate regimes. With these three assumptions in mind we can discuss the crossover between the mushroom and the brush regimes as they occur on a surface imposing homogeneous anchoring. The situation differs from that for homeotropic anchoring because we now have two radii of gyration, $R_\parallel$ and $R_\perp$,[26] in the plane of the surface. For low coverages $\Sigma \gg R_\parallel^2$ the layer consists of noninteracting cigar-shaped chains (Figure 4a). When the overlap threshold is reached, $\Sigma_0 \approx R_\parallel^2$, the cigars begin to overlap along the parallel direction, but not in the perpendicular direction. A series of parallel, semicylindrical brushes is thus obtained (Figure 4b). An Alexander model incorporating the Flory exponents yields the following free energy per chain

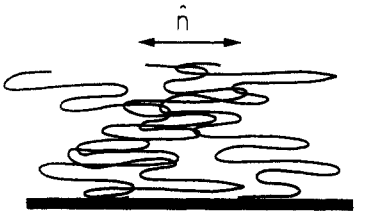

Figure 5. A nontilted, homogeneously anchored brush depicted according to the Alexander model.

$$F/kT = v_n \frac{N^2}{H^2\Sigma^{1/2}} + \frac{H^2}{Nal} \tag{33}$$

where H is the brush height, which in this case is identical to the radius of the cylinder. In equilibrium H is

$$H \approx (v_n al)^{1/4} N^{3/4} \Sigma^{-1/8} \tag{34}$$

As expected this is, essentially, the familiar expression for the radius of a cylindrical brush of isotropic chains.[32,33] It is also close to the free chain radius, $R_\perp$ (26), for $\Sigma = \Sigma_0 = R_\parallel^2$. For larger grafting densities the cylinders begin to overlap laterally (Figure 4c). This occurs at $H \approx \Sigma^{1/2}$ or $\Sigma^* \approx (v_n al)^{2/5} N^{6/5}$. Σ^* thus obtained is comparable to the intuitive value $R_\parallel R_\perp = (val)^{2/5}(l/a)^{11/10} N^{6/5} \exp(3U_h/20kT) = (l/a)^{11/10} \exp(3U_h/20kT)\Sigma^*$. This is because the "cylindrical" regime, which occurs for $\Sigma^* < \Sigma < \Sigma_0$, the interaction energy is lowered by lateral swelling. Similar behavior may be obtained from flexible, isotropic chains which are grafted anisotropically. However, one should note that disorder in the spatial arrangement of the grafting sites may have a significant effect on this regime. For coverages greater than a^2/Σ^* the cigars overlap in both directions. Consequently lateral swelling is no longer beneficial and all swelling takes place perpendicular to the surface.

For $\Sigma < \Sigma^*$ a simple analysis is possible when chain tilt is not allowed (Figure 5). In this case we have

$$F = v_n N^2/\Sigma H + H^2/Ll \tag{35}$$

and the equilibrium layer thickness is

$$H_{\parallel 0} \approx v_n^{1/3} N(al/\Sigma)^{1/3} \tag{36}$$

Both $H_{\parallel 0}$ (28) and $H_{\perp 0}$ retain the Alexander scaling behavior as obtained for brushes of flexible chains in isotropic solvents; i.e., $H \approx v^{1/3} N(a^2/\Sigma)^{1/3}$. Note however that v_n replaces v and al replaces a^2. Comparison between $H_{\parallel 0}$ and $H_{\perp 0}$ reveals a distinctive feature of these brushes: The layer thickness in the homeotropic case is much thicker, $H_{\parallel 0} \ll H_{\perp 0}$. Furthermore, $H_{\parallel 0}$ exhibits an exponential temperature dependence which is absent in $H_{\perp 0}$. The fact that $H_\perp$ is much larger than that for an isotropic brush suggests the following simple experiment (Figure 2). A brush is grafted to a surface imposing homeotropic anchoring. When the system is in the high temperature isotropic phase, the brush is simply an isotropic brush of height $H_I \approx v^{1/3} N(a^2/\Sigma)^{1/3}$. We now cool into the nematic state, whereupon the brush undergoes a rapid expansion to a state $H_\perp \approx v_n^{1/3} N(al/\Sigma)^{1/3} \exp(U_h/3kT) \gg H_I$.

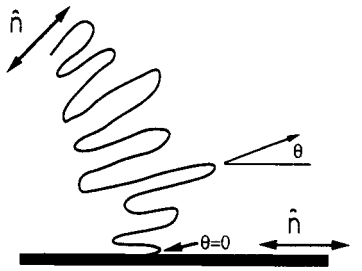

Figure 6. One tilted chain in a homogeneously anchored brush. The tilt increases gradually from $\theta = 0$ at the surface to its maximal value at the boundary of the layer.

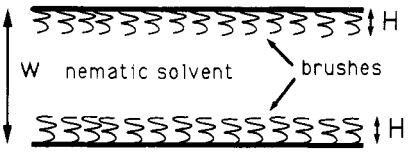

Figure 7. Two-brush geometry used in the calculations for a homogeneously anchored brush.

Our preceding analysis is deficient because it ignores chain tilt which enables the system to lower its free energy further. Repulsive monomer–monomer interactions grow in importance as the grafting density increases. Tilt provides a mechanism for increasing H thus lowering ϕ and F_{int} (Figure 6). Two effects are involved. The first is purely geometrical. The homogeneous anchoring aligns the cigar-like LCPs with the surface. Tilting their long axes with respect to the surface will increase H even if the dimensions of the LCP remain fixed. As it happens, tilt favors swelling beyond this geometrical effect. In the absence of tilt the restoring force is due to the Gaussian $F_{el}(R_\perp)$. For finite tilt the restoring force is due to a vector sum of contributions originating with both $F_{el}(R_\perp)$ and the softer $F_{el}(R_\parallel)$. As a result the restoring force is weakened thus promoting further swelling of the layer. At the same time tilt gives rise to a free energy penalty due to the associated distortion of the nematic medium. Because of the interplay of these two factors, the tilt takes place as a second-order phase transition. It is possible to extend the Alexander model so as to allow for chain tilt. A continuum description is adopted for the nematic distortion. The orientation of $\mathbf{n}$ within the layer is assumed to vary continuously with z, the distance from the surface. At each altitude the tilt is translationally invariant so that the director field is specified by the tilt angle $\theta(z)$. Because of the homogeneous anchoring conditions $\theta(0) = 0$. $\theta(z)$ reaches its maximum value, $\theta(H)$, at the upper boundary of the layer. For simplicity we consider the symmetric case of a nematic solvent bounded between two identical brushes (Figure 7). In this case the tilt angle in the bulk is constant, set by the boundary of the brush, $\theta(H)$. The variation of $\theta(z)$ within the layer is described by the trial function

$$\theta(z) = Q \sin(\pi z/2H) \qquad 0 < z < H \tag{37}$$

Q, the variational parameter, also serves as the order parameter of the system. The director field within the layer is specified by $\mathbf{n} = (\cos\theta, \sin\theta)$. The distortion free energy, as obtained from (1) by using this $\mathbf{n}$ and the one constant approximation, is

$$F_{dis} = (\Sigma K/2)\int_0^H (d\theta/dz)^2\, dz\ (\pi^2/16)(\Sigma K/H)Q^2 \tag{38}$$

where K is the elastic constant of the nematic.

The trajectory of the LCPs locally follows $\mathbf{n}$. However, in the framework of the Alexander model the polymer is described in terms of its average characteristics. Accordingly we view the LCP as interpenetrating ellipsoids with uniform tilt angle, $\bar{\theta}$, given by

$$\bar{\theta} = \frac{1}{H}\int_0^H \theta(z)\, dz \tag{39}$$

Ignoring numerical prefactors we relate $\bar{\theta}$ to the layer thickness via

$$H = R_\parallel \sin\bar{\theta} + R_\perp \cos\bar{\theta} \tag{40}$$

This, together with the original assumptions of the Alexander model, specifies the polymeric contribution to the free energy per chain: $F_{int} + F_{el}(R_\parallel) + F_{el}(R_\perp)$. Because of the tilt, it is necessary to allow for the extension of both $R_\parallel$ and $R_\perp$. Altogether, the total free energy per chain, including the nematic distortion term, $F_{chain} = F_{dis} + F_{int} + F_{el}(R_\parallel) + F_{el}(R_\perp)$, is

$$F_{chain}/kT = \frac{\pi^2}{16}\frac{\Sigma K}{kTH}Q^2 + \upsilon_n\frac{N^2}{\Sigma H} + \frac{R_\perp^2}{R_{\perp 0}^2} + \frac{R_\parallel^2}{2R_{\parallel 0}^2} \tag{41}$$

where we have assumed that the Gaussian limit of $F_{el}(R_\parallel)$ applies. We emphasize here that we adopt a scaling approach, so that the numerical coefficients in the free energy should not be taken too seriously. We first minimize F_{chain} with respect to H and $R_\parallel$ thus obtaining H, $R_\parallel$, and $R_\perp$ as functions of Q. This allows us to write the free energy in terms of two dimensionless variables, $\mu = (R_{\perp 0}/R_{\parallel 0})$ and $\alpha = (K\sigma/2kTH_{\parallel 0})(R_{\perp 0}/H_{\parallel 0})^2$. The height of the brush in the absence of tilt is

$$H_{\parallel 0} = \frac{\mu^{2/3}N^{2/3}R_{\parallel 0}^{2/3}\upsilon^{1/3}}{2^{1/3}\Sigma^{1/3}} \tag{42}$$

This has an exponential temperature dependence through $R_{\parallel 0}$. The free energy reduces to the simple expression

$$F_{chain} \propto \frac{(16 + \alpha\pi^2Q^2)^{2/3}}{[\mu^2 + 2 + (\mu^2 - 2)\cos(4Q/\pi)]^{1/3}} \tag{43}$$

α is roughly $\alpha \approx F_{dis}(Q=1)/F_{el}(R_\perp(Q=0))$. When $\alpha < \alpha_c$ the distortion penalty of the nematic is dominant and the system is not expected to tilt. In the opposite case, $\alpha > \alpha_c$, the deformation free energy of the LCP is important and tilt is beneficial. To study the onset of tilt, we investigate the Landau expansion with respect to Q about $Q = 0$. This yields

$$F_{chain} \propto F_0 + (\alpha - \alpha_c)Q^2 + BQ^4 + CQ^6 \tag{44}$$

where F_0 is F_{chain} for the untilted state, $Q = 0$.

$$\alpha_c = (32/\pi^4)(2\mu^{-2} - 1) \tag{45}$$

Both B and C are complicated functions of α and μ, and can be obtained from (43) by differentiating. While B is positive, C is negative in the region of interest (contrary to the claim in our earlier publication[24]). A standard analysis,[45] which is applicable when the last term is small, identifies the change in the sign of the quadratic term with a second-order phase transition at $\alpha = \alpha_c$. This is confirmed by numerical analysis of the full free energy (43), (Figure 8). $R_\parallel/H_{\parallel 0} \approx (4/\pi)\mu^{-2}Q$ always increases with the tilt. $R_\perp/H_{\parallel 0} \approx 1 - (2/\pi^2)Q^2[1 + (4\alpha_c - \alpha)\pi^4/96]$ decreases with Q when $\alpha < \alpha_c$. As expected $H/H_{\parallel 0} \approx 1 + (\pi^2/48)Q^2(1 + 2\alpha_c)$ also increases with Q in this regime. While the anchoring condition at the interface remains unchanged, the director angle at the outer edge of the brush shifts from $\theta(H) = 0$ to a finite $\theta(H)$. This effect is independent of the separation between the brushes. It can take place in a single brush immersed in a reservoir of nematic solvent. It is, accordingly, a form of an anchoring transition.[31] A

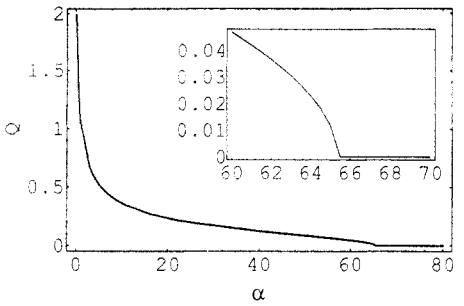

Figure 8. A plot of the order parameter Q, which is proportional to the tilt angle $\bar{\theta}$ *vs* α, which measures the relative importance of the bulk nematic distortion and the chain elastic penalty, for $\mu = R_{\perp 0}/R_{\parallel 0} = 0.1$. At large α, $>\alpha_c$ ($\alpha_c \approx 65$ for $\mu = 0.1$) the system is untilted. At $\alpha = \alpha_c$ the chain elasticity begins to dominate the system and it undergoes a second-order tilting phase transition. As α decreases below α_c, the tilt angle gradually increases. For very small α the order parameter approaches the unphysical value $Q = \pi^2/4$ because the approximations used break down. The insert is a magnified view of the region near α_c, showing the typical, square root behavior of the order parameter near the transition. The plot was made by minimizing the "exact" free energy (43).

few examples of such transitions, of first and second order, were experimentally observed. However, their microscopic origin, in these cases, is not clear.

V. Confined Brushes: A Frederiks-like Transition

It is straightforward to generalize the analysis of the previous section to the case of LCP brush subject to compression. The situation we envision involves compression of two identical brushes. Our primary focus is on the confinement of brushes grafted onto surfaces imposing homeotropic alignment. We invoke the impenetrability ansatz:[32,33] Two compressed brushes exhibit negligible interpentration and their thickness thus equals half of the slit width. The free energy in dimensionless form follows directly from (41). Since the height H is fixed, we need only minimize with respect to $R_\parallel$. This yields

$$F_{\text{chain}} \propto (16\mu^2 + \alpha\pi^2\mu^2Q^2 + 8\mathcal{S}^2\mu^2\eta^3 + \mathcal{T}^2[32 + 2\alpha\pi^2Q^2])(\mu^2 + 2\mathcal{T}^2)^{-1} \quad (46)$$

where $\eta = H/H_{\parallel 0} < 1$, $\mathcal{T} = \tan(2Q/\pi)$, and $\mathcal{S} = \sec(2Q/\pi)$. $H_{\parallel 0}$ is the height of the brush in the absence of compression and tilt (42). The critical value of α at which the second-order tilting transition occurs in this case is

$$\alpha_c^*(H) = \alpha_c H^3/{H_{\parallel 0}}^3$$

where α_c is given by (45). As a result the critical grafting area per chain

$$\Sigma_c(H) \sim \frac{kT}{K}\frac{{R_{\parallel 0}}^2}{{R_{\perp 0}}^4}H^3 \quad (47)$$

exhibits a strong dependence on the brush compression.

In an earlier work[28,29] we studied the confinement of free LCP in a nematic θ solvent to slit imposing homeotropic anchoring. A similar tilting phase transition was found. It was driven by the competition between the confinement induced deformation penalty of the polymer and the distortion energy of the bulk nematic. For strong confinement, the polymer and the bulk nematic tilt. The system gains partial relief of the polymer deformation at the price of a nematic distortion penalty. Although this polymer was not grafted, it is possible to extract a critical area per chain of

$$\Sigma_c = \frac{kT}{K}\frac{{R_{\parallel 0}}^2}{H}\left[1 - \left(\frac{H}{R_{\parallel 0}}\right)^2\right] \quad (48)$$

In this case tilt is favored for strong compressions. In a Θ solvent $R_\parallel$ and $R_\perp$ are decoupled and hence $R_\perp$ does not appear in the expression for Σ_0.

Finally, note that the effect of confinement depends on the anchoring conditions. It promotes tilting in the homeotropic case. However, compression is expected to repress tilt in a brush subject to homogeneous anchoring.

VI. The Effect of External Fields

Liquid crystalline molecules exhibit anisotropy of the magnetic susceptibility and dielectric constants. Accordingly, electric and magnetic fields can align the liquid crystalline medium. Interesting situations occur when the orientation imposed by the bounding surfaces is not consistent with the alignment induced by the field. The competition between the two effects can give rise to a nematic distortion which takes place as a second-order phase transition known as the Frederiks transition.[25-27] This phenomenon is heavily utilized in the design of liquid crystalline displays.[30] In the following we combine the field-driven Frederiks transition with the anchoring transition considered above. As we have seen, the anchoring transition is driven by the interaction penalty of the LCP. It is controlled by the grafting density and the confinement of the brush. The combination of the two effects provides new routes to control the onset of the nematic distortion. As such, this combined system may be of technological interest. For specificity we consider a slab of low molecular weight, monomeric nematic in a slit imposing homogeneous anchoring. The magnetic susceptibilities, $\chi_\parallel$, $\chi_\perp$, parallel and perpendicular to the director, are chosen so that $\Delta\chi = \chi_\parallel - \chi_\perp > 0$. This implies that the nematic director favors parallel alignment to the applied magnetic field. Clearly no distortion occurs if the applied field, $\mathcal{B}$, is parallel to the bounding surfaces. A Frederiks transition is expected when the applied field is perpendicular to the slit surface. The alignment imposed by the anchoring is dominant for weak fields. When the field strength increases beyond a critical value, $\mathcal{B}_c$, the bulk is aligned by the field while the anchoring conditions at the boundaries are still obeyed. As a result a sigmoid distortion develops. The critical field, $\mathcal{B}_c \approx (\pi/W)(K/\Delta\chi)^{1/2}$, is set by the balance of the magnetic and distortion energies of the nematic. Apart from material constants, the elastic constant, K, and the magnetic susceptibility, $\Delta\chi$, $\mathcal{B}_c$ depends on the layer thickness, W. W is thus the only control parameter for a given temperature and working material. We now incorporate into the system LCP brushes grafted onto both surfaces. For simplicity we assume that $\chi_\parallel$ and $\chi_\perp$ of the LCP and of the monomeric solvent are identical. This system has two extra control parameters: Σ and N. When Σ is below the overlap threshold, one expects the familiar Frederiks transition. For $\Sigma < \Sigma_c$ the anchoring transition will occur in the absence of an external field. An interesting effect is expected when $\Sigma > \Sigma_c$ but $\Sigma \approx \Sigma_c$. In this regime the tilting transition of the bulk nematic and the anchoring transition in the brush occur simultaneously. Furthermore, it is possible to tune the critical magnetic field $\mathcal{B}_c$ by adjusting the grafting density. In particular, the critical field can be made arbitrarily small by choosing the grafting density just below, but close to, its critical value.

As before the nematic director is described by a trial function. However, in this case it is necessary to allow for different distortions inside and outside the brush. Consequently, two order parameters, Q_1 and Q_2, come into play. Inside the brushes we use

$$\theta(z) = Q_1 \sin[\pi z/2H] \qquad (49a)$$

$$z < H \qquad W - H < z < W$$

and in the bulk

$$\theta(z) = Q_1 + Q_2 \sin[\pi(z - H)/(W - 2H)] \qquad (49b)$$

$$H < z < W - 2H$$

This provides a trial function which is continuous across the brush boundary and which reduces to the exact Frederiks transition[25-27] distortion in the appropriate limits. Note that when $Q_2 = 0$ and $Q_1 \neq 0$, the brush is tilted and distorted, but the bulk is just tilted. Bulk distortion occurs for $Q_2 \neq 0$. The nematic distortion term per chain when $Q_1 \neq 0$ and $Q_2 \neq 0$ is

$$F_{dis}/kT = (\pi^2/16)(\Sigma K/kTH)(2H - W)^{-1}[(2H - W)Q_1^2 - 2HQ_2^2] \qquad (50)$$

and the magnetic term is

$$F_M/kT = -(\Sigma\Delta\chi\mathcal{B}^2/2kT)\int_0^{W/2} dz \sin^2\theta \qquad (51)$$

Accordingly, the total free energy, $F_{chain} = F_{dis} + F_{int} + F_{el}(R_\parallel) + F_{el}(R_\perp) + F_M$, is

$$F_{chain}/kT = (\pi^2/16)(\Sigma K/kTH)(2H - W)^{-1}[(2H - W)Q_1^2 - 2HQ_2^2] + \upsilon_n\frac{N^2}{\Sigma H} + \frac{R_\perp^2}{R_{\perp 0}^2} + \frac{R_\parallel^2}{2R_{\parallel 0}^2} - (\Sigma\Delta\chi\mathcal{B}^2/2kT)\int_0^{W/2} dz \sin^2\theta \qquad (52)$$

We now restrict the analysis to the case of small Q_1 and Q_2, and thus explicitly study only the vicinity of the second-order phase transition. Even with this restriction the algebra is far from simple. Expanding to second order in Q_1 and Q_2 yields

$$F_{chain}/kT = (\pi^2/16)(\Sigma K/kTH)(2H - W)^{-1}[(2H - W)Q_1^2 - 2HQ_2^2] + \upsilon_n\frac{N^2}{\Sigma H} + \frac{1}{\mu^2 R_{\parallel 0}^2}\left[H^2 - \frac{4HR_\parallel}{\pi}Q_1 + \left(\frac{4H^2}{\pi^2} + \frac{4R_\parallel^2}{\pi^2}\right)Q_1^2\right] + \frac{R_\parallel^2}{2R_{\parallel 0}^2} - (\Sigma\Delta\chi\mathcal{B}^2/2kT)\left[Q_1^2\left(\frac{W}{2} - \frac{H}{2}\right) + Q_2^2\left(W/4 - \frac{H}{2}\right) + Q_1Q_2\left(\frac{2W}{\pi} - \frac{4H}{\pi}\right)\right] \qquad (53)$$

The condition $\partial F_{chain}/\partial R_\parallel = 0$ allows us to eliminate $R_\parallel$ from (53) leading to F_{chain} which depends on H alone

$$F_{chain}/kT = F_0(H)/kT + Q_1^2A(H) + Q_2^2B(H) + Q_1Q_2C(H) \qquad (54)$$

The coefficients are

$$A = (\omega - 2h)(32\mu^2 + 4\alpha h^2\mu^2\pi^2 - 4\alpha h\mu^2\omega\pi^2 + \alpha\mu^2\pi^4 - 64) \qquad (55)$$

$$B = 2\alpha h\mu^2\pi^2((2h - \omega)^2 - \pi^2) \qquad (56)$$

and

$$C = -16\alpha h\mu^2(\omega - 2h)^2\pi \qquad (57)$$

where $h = H/\xi_B$, $\omega = W/\xi_B$, and ξ_B is the magnetic correlation length $\xi_B = (K/\Delta\chi)^{1/2}\mathcal{B}^{-1}$. Note that $h < \omega/2$ because the brushes are assumed not to interpenetrate. It is impossible to analytically eliminate H from (54) by using $\partial F_{chain}/\partial H = 0$. However, since we are only interested in F_{chain} in the vicinity of the phase transition, Q_1 and Q_2 are small and $H \approx H_0$ where H_0, given by (42), is the layer thickness in the absence of tilt. We can thus solve for $\delta \ll H_0$, where $H = H_0 + \delta$, so as to eliminate δ from the expression. To this end we make use of $(\partial F_0/\partial H)|_{H=H_0} = 0$. To lowest order in the Q's, $F'(H) \equiv \partial F/\partial H = 0$ gives

$$\delta \approx -(Q_1^2A'(H_0) + Q_2^2B'(H_0) + Q_1Q_2C'(H_0))/F_0''(H_0) \qquad (58)$$

This, together with (54), yields

$$F_{chain}/kT \approx Q_1^2A(H_0) + Q_2^2B(H_0) + Q_1Q_2C(H_0) \qquad (59)$$

The untilted brush is stable when F_{chain}, as given by (59), is positive definite. It is thus necessary to identify the values of μ, α, ω, and h for which (59) is positive for all $Q_1 > 0$ and $Q_2 > 0$. This condition is fulfilled when the eigenvalues of the matrix

$$\begin{pmatrix} A & C/2 \\ C/2 & B \end{pmatrix} \qquad (60)$$

are positive. Accordingly, the untilted phase is stable when (i) $A > 0$ and (ii) $4AB - C^2 > 0$. For $C = 0$, A controls the phase transition of Q_1 and B that of Q_2. In such a case the bulk and brush transitions would take place independently. However, because $C > 0$, it couples the order parameters Q_1 and Q_2. As a result the phase transitions must occur simultaneously for both Q_1 and Q_2; i.e., the eigenvectors of (60) have nonzero Q_1 and Q_2 components. Physically, the tilt in the brush occurs at the same time as the nematic distortion in the bulk. An ordinary Fredericks transition is expected when $\omega > \pi$, since the presence of the brush can only make the transition easier. Indeed, for $\omega > \pi$, $4AB - C^2 < 0$. Of greater interest is the case of a brush much thinner than the slab $h \ll \omega \ll \pi$. In this regime tilting occurs when $A = 0$. This condition yields for the critical field

$$\mathcal{B}_c/\mathcal{B}_c^\circ = \frac{1}{2}(W/H_c^\circ)^{1/2}[1 - (\Sigma_c^\circ/\Sigma_c)^{-2}]^{1/2} \qquad (61)$$

where B_c° is the critical tilting field in the absence of a brush, Σ_c° is the critical grafting area in the absence of a field, and H_c° is the height of the brush at $\Sigma = \Sigma_c^\circ$ with no field. This is one main important result of the paper (Figure 9). In the absence of a brush the Frederiks transition occurs when $\mathcal{B}_c = \pi/W(K/\Delta\chi)^{1/2}$. In liquid crystal display devices, it is beneficial to decrease W so as to have faster response. However, this means that $\mathcal{B}_c$, or equivalently, the critical electric field, must be large. By grafting a PLC brush to both surfaces, we can lower the critical field to arbitrarily small values (61).

VII. Conclusion

The configuration of flexible chains in isotropic media are well explained in terms of entropic elasticity and monomer–monomer interactions.[4] The dominant factors for LCPs in nematic media are the chain rigidity and the anisotropic interactions between the chain segments and the nematic field. The role of monomer–monomer interactions, while important, is less crucial. Short LCPs tend to be fully extended, exhibiting only lateral undu-

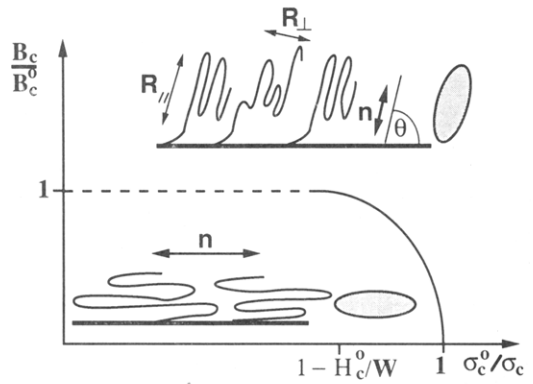

Figure 9. Critical field, $\mathcal{B}_c$, for the Frederiks type transition in a cell coated by brushes. $\mathcal{B}_c$ is plotted against the critical grafting density, $1/\Sigma_c$, for the case where the brush height is much less than the plate separation. Below the curve the entire system is aligned parallel to the boundary (lower inset). Above the curve, tilting takes place (upper insert). When $\Sigma_c^0/\Sigma_c < 1 - H_c^0/W$, a normal Frederiks transition takes place (dotted line). Near Σ_c^0, the driving force for the anchoring transition is significant and $\mathcal{B}_c$ decreases. The ellipsoids illustrate the overall shape and orientation of the chains.

lations. The lateral chain dimension can be characterized as that of a two-dimensional random walk of step l, $R_{\perp 0}^2 \approx (L/l)l^2$. Long LCPs are qualitatively different. They support hairpin defects which allow the chain trajectory to reverse its direction. The hairpins are excitations which are entropically favorable but energetically penalized. Consequently, their equilibrium number has a characteristic Boltzmann form. This, in turn, is the origin of the distinctive exponential temperature dependence of traits due to the presence of hairpins. Because of the hairpins, long LCPs may be envisioned as prolate ellipsoids. As in short LCPs, the lateral dimension, the minor axis, is controlled by the lateral undulations so that $R_{\perp 0}^2 \approx (L/l)l^2$. The behavior of the major axis, $R_\parallel$, is qualitatively different. $R_\parallel$, is much shorter than L because the hairpins give rise to a one-dimensional random walk component so that $R_\parallel \approx n_0(L/n_0)^2$. This anisotropy also characterizes the deformation behavior of the main chain LCPs. The deformation of $R_\perp$ gives rise to the familiar Gaussian free energy penalty. In marked contrast, the extension of $R_\parallel$ is associated with a distinctive Ising elasticity. This is traceable to the nonconservation of hairpins as discussed in section III. At small extensions of $R_\parallel$ an ordinary Gaussian behavior is obtained. However at larger extensions we rapidly enter a regime where nonlinear corrections are important. This regime is much more accessible than the corresponding regime in isotropic polymers. In particular, the nonlinear regime is expected to affect the rheology of LCPs; the behavior of LCP brushes and aggregates of block copolymers containing LCP blocks, and, finally, the elasticity of networks and gels produced from main chain LCPs.

As noted above, monomer–monomer interactions are less dominant in our system than in isotropic polymers. The extended configurations adopted by short LCP tend to repress such interactions. They regain some importance for long LCPs which support many hairpins. A Flory type theory of swelling, described in section III, suggests that $R_\parallel$ and $R_\perp$ of such chains exhibit the familiar Flory $N^{3/5}$ scaling. The shape anisotropy is retained because of prefactors giving rise to exponential temperature dependence. These cause $R_\parallel$ to *shrink* with increasing T while $R_\perp$ *grows*. The observation of this swelling behavior by SANS experiments should be easier than the corresponding experiments on melts of LCPs. Since the melting point of such solutions is set, primarily, by the nematic solvent, there is no need for elevated temperatures. Consequently, the transesterification problem is not as important. Also, the preparation of uniform samples is not as demanding.

The discussion of the single, free LCP coils involves novel concepts with no counterpart in the behavior of the familiar flexible polymers. The predicted configurations are, however, more routine. Swollen LCPs exhibit the familiar Flory $N^{3/5}$ scaling. The shape anisotropy by itself is not that distinctive since it has been argued that flexible chains in isotropic media are also cigar-like objects.[51] Finally, the distinctive Ising elasticity does not come into play for free LCPs in equilibrium situations. On the other hand, LCPs in a nematic medium are distinct in that they may be oriented in space by aligning the liquid crystal as a whole. In turn, this enables the measurement of $R_\parallel$ and $R_\perp$. This very effect, the orientation of LCPs by an aligned nematic solvent gives rise to qualitatively novel interfacial effects. LCPs which are constrained to a slit or grafted to a surface may be oriented by the alignment imposed by the surface. At the same time one may increase the free energy of the chain by geometrical confinement or by increased overlap with neighboring chains. In certain cases, the system can lower its total free energy by tilting, thus alleviating the chain penalities at the price of a nematic distortion. As was discussed in sections VI–IV, this takes place as a second-order tilting phase transition. Neither the tilt nor the associated phase transition have counterparts in the behavior of flexible polymer in isotropic media.

In the case of isotropic brushes, the Alexander model was followed by a more precise self-consistent field (SCF) description.[32,33] The SCF theory provides more detailed information on the concentration profile and the distribution of free ends. It is desirable to extend the SCF approach to the case of LCP brushes. A first step in this direction was already taken by Pickett and Witten[52] who considered brushes of LCP in melt conditions. However, the extension of the SCF description to LCP brushes in a nematic solvent is much more difficult in the presence of tilt. The formulation of the SCF theory begins with a local free energy density of a chain in the brush. For an isotropic brush the elastic term for a chain stretched in the z direction is simply $(dz/dn)^2\, dn$. For tilted LCP brushes it is necessary to account for two elastic contributions due to both the Ising and Gaussian elasticities. This suggests that the elastic free energy per chain in such brushes may be written as

$$f_{el}/kT = \int_0^N dn\left[\frac{1}{al}\left(\frac{dr_\perp}{dn}\right)^2 + \frac{1}{al\exp(U/kT)}\left(\frac{dr_\parallel}{dn}\right)^2\right] \quad (57)$$

where the perpendicular distance traversed by the chain is

$$dz = \cos\theta\, dr_\perp + \sin\theta\, dr_\parallel \quad (62)$$

and θ is the angle made by the chain trajectory with the horizontal plate. However, the detailed implementation of such an SCF calculation is beyond the scope of this paper.

Acknowledgment. D.R.M.W. and A.H. enjoyed financial support provided by DOE Grant DE-FG03-87ER45288 and the Ford Motor Co. Part of this work was carried out while D.R.M.W. was in Santa Barbara. The authors thank J. Israelachvili and P. Pincus for helpful discussions.

References and Notes

(1) Volino, F.; Gauthier, M. M.; Giroud-Godquin, A. M.; Blumstein, R. B. *Macromolecules* **1985**, *18*, 2620.

(2) Volino, F.; Blumstein, R. B. *Mol. Cryst. Liq. Cryst.* **1984**, *147*, 113.
(3) D'Allest, J. F.; et al. *Phys. Rev. Lett.* **1988**, *61*, 2562.
(4) de Gennes, P. G. *Scaling Concepts in Polymer Physics*; Cornell University Press: Ithaca, NY, 1979.
(5) Alexander, S. J. *Phys. (Paris)* **1977**, *38*, 977.
(6) de Gennes, P. G. In *Polymer Liquid Crystals*; Ciferri, A., Krigbaum, W. R., Meyer, R., Eds.; Academic Press: New York, 1982.
(7) Gunn, J. M. F.; Warner, M. *Phys. Rev. Lett.* **1987**, *58*, 393.
(8) Warner, M.; Gunn, J. M. F.; Baumgartner, A. B. *J. Phys. A: Math. Gen.* **1985**, *18*, 3007.
(9) Williams, D. R. M.; Warner, M. *J. Phys. (Paris)* **1990**, *51*, 317.
(10) Williams, D. R. M.; Warner, M. In *Computer Simulation of Polymers*; Roe, R. J., Ed.; Prentice Hall: Englewood Cliffs, NJ, 1991.
(11) Le Doussal, P.; Nelson, D. R. *Europhys. Lett.* **1991**, *15*, 161.
(12) Croxton, C. A. *Macromolecules* **1991**, *24*, 537.
(13) Toner, J. *Phys. Rev. Lett.* **1992**, *68*, 1331.
(14) Williams, D. R. M. *J. Phys. A* **1991**, *24*, 4427.
(15) Selinger, J. V.; Bruinsma, R. F. *J. Phys. II* **1992**, *2*, 1215.
(16) Warner, M.; Williams, D. R. M. *J. Phys. II* **1992**, *2*, 471.
(17) Warner, M.; Gelling, K. P.; Vilgis, T. A. *J. Chem. Phys.* **1988**, *88*, 4008.
(18) Kamien, R. D.; Le Doussal, P.; Nelson, D. R. *Phys. Rev. A* **1992**, *45*, 87227.
(19) Flory, P. *Principles of Polymer Chemistry*; Cornell University Press: Ithaca, NY, 1953.
(20) Flory, P. *Statistical Mechanics of Chain Molecules*; Wiley: New York, 1969.
(21) D'Allest, J. F.; et al. *Phys. Rev. Lett.* **1988**, *61*, 2562.
(22) Arrighi, V.; Higgins, J. S.; Weiss, R. A.; Cimecioglu, A. L. *Macromolecules* **1992**, *25*, 5297.
(23) Li, M. H.; Brûlet, A.; Davidson, P.; Keller, P.; Cotton, J. P. *Phys. Rev. Lett.* **1993**, *70*, 2297.
(24) Halperin, A.; Williams, D. R. M. *Europhys. Lett.* **1993**, *21*, 575.
(25) de Gennes, P. G. *The Physics of Liquid Crystals*; Clarendon: Oxford, 1974.
(26) Chandrasekhar, S. *Liquid Crystals*; Cambridge University Press: Cambridge, 1977.
(27) Vertogen, G.; de Jeu, W. H. *Thermotropic Liquid Crystals, Fundamentals*; Springer Verlag: Berlin, 1988.
(28) Williams, D. R. M.; Halperin, A. *Europhys. Lett.* **1992**, *19*, 693.
(29) Williams, D. R. M.; Halperin, A. *Macromolecules* **1993**, *26*, 2025.
(30) Bahadur, B., Ed. *Liquid Crystals Applications and Uses*; World Scientific: Singapore, 1990.
(31) Jerome, B. *Rep. Prog. Phys.* **1991**, *54*, 391.
(32) For a review see Halperin, A.; Tirrell, M.; Lodge, T. *Adv. Polym. Sci.* **1992**, *100*, 33, and the following reference.
(33) Milner, S. T. *Science* **1991**, *251*, 905.
(34) Halperin, A.; Williams, D. R. M. *Europhys. Lett.* **1992**, *20*, 601.
(35) The nematic order is more accurately represented by a symmetric traceless rank-2 tensor. This complication plays no role in the simplified analysis presented here.
(36) Brochard, F. *J. Phys. (Paris)* **1979**, *40*, 1049.
(37) Equation 2 is an expansion for small S. We are usually interested in the large S limit, where (2) may become somewhat inaccurate.
(38) Vroege, G. J.; Odijk, T. *Macromolecules* **1988**, *21*, 2848.
(39) de Gennes, P. G. In *Polymer Liquid Crystals*; Ciferri, A., Krigbaum, W. R., Meyer, R., Eds.; Academic Press: New York, 1982.
(40) Odijk, T. *Macromolecules* **1986**, *19*, 2313.
(41) For a review see Kokhlov, A. R.; Semenov, A. N. *Sov. Phys. Usp.* **1988**, *31*, 988.
(42) MacDonald, W. A.; McLenanghan, A. D. W.; Richards, R. W. *Macromolecules* **1992**, *25*, 826.
(43) Richardson, J. S. *Adv. Protein Chem.* **1981**, *34*, 167.
(44) Ma, S. K. *Statistical Mechanics*; World Scientific: Philadelphia, PA, 1985.
(45) Huang, K. *Statistical Mechanics*; J. Wiley: New York, 1987.
(46) In practice, at low hairpin densities the hairpins obey Boltzmann statistics.
(47) Margenau, H.; Murphy, G. M. *The Mathematics of Physics and Chemistry*; Van Nostrand: New York, 1956.
(48) Hill, T. L. *An Introduction to Statistical Thermodynamics*; Addison-Wesley: Reading, MA, 1960.
(49) Williams, D. R. M., *J. Phys. A.* **1991**, *24*, 4427.
(50) Lai, P.-Y.; Halperin, A. *Macromolecules* **1991**, *24*, 4981.
(51) Aronovitz, J. A.; Nelson, D. R. *J. Phys. (Paris)* **1986**, *47*, 1445.
(52) Pickett, G. T.; Witten, T. A. *Macromolecules* **1992**, *25*, 4569.